Hindawi
Wireless Communications and Mobile Computing
Volume 2021, Article ID 7192484, 12 pages
https://doi.org/10.1155/2021/7192484

Research Article

Drive System Design for Small Autonomous Electric Vehicle: Topology Optimization and Simulation

Zhongming Wu, Mufangzhou Zhu, Yu Guo, Li Sun, and Yuchen Gu

Department of Mechanical and Electrical Engineering, Jinling Institute of Technology, Nanjing 211169, China

Correspondence should be addressed to Zhongming Wu; wuzhming0926@163.com

Received 30 September 2021; Accepted 3 November 2021; Published 16 December 2021

Academic Editor: Deepak Gupta

High driving efficiency remains challenging in autonomous electric vehicles, especially in small electric vehicle subtype. Here, we reported investigation of the structure and requirements of the drive system for those vehicles, while the motor-drive axle combined integrated driving scheme has been chosen. In the study, the power matching of drive motor as well as transmission ratio has been calculated based on the performance of the small electric vehicles, and the total gear ratio of 8.124 was determined. For better comprehensive performance and efficiency, the two-stage retarder has been designed, in which elements including high-speed shaft, low-speed shaft, gears, and differential have been examined to ensure their proof strength when the motor outputs reached the maximum torque. Notably, by utilizing topology optimization, Gear 4, the transmission unit with the heaviest weight percentage has been modified in a lightweight way, achieving a 41% reduction of the mass in emulation analysis and turned up to the target of optimization eventually.

1. Introduction

Energy conservation and environmental protection remain a great global social concern, with great attention on the development and applications of energy-saving and emission reduction technology in the industry and daily life. It is widely accepted in the reduction of carbon emission, and thus, particular carbon emission management has been established in some countries and regions. Fossil fuels are the common energy resources for traditional vehicles, which has been identified as the pivotal field for carbon emission governance. Currently, energy-saving and emission reduction technology leads the development of vehicles, in which technology for new energy vehicles holds priority by research institutions and auto enterprises. Compared to conventional fossil-fueled cars, electric vehicles hold various advantages, such as zero-carbon, heralding vast potentials for application, and considerable market prospects, whereas the rapid technology development has been achieved by auto industries.

The drive system, one of the essential units in electric vehicles, directly influences the vehicles' performance and efficiency, indicating the necessity of the particular optimization in compacting structure for better match of the driving motor. Ample of studies have shown the simpler and more compact driving system in electric cars than in patrol-driven cars.

Hence, the study was designed to reduce the mass and volume of the driving system for the improvement of transmission efficiency and further reduction of energy consumption under the ensurance of reliable properties. Based on previous studies, we designed the transmission system of the electric vehicles and optimized the driving system by reducing the weight of transmission units following the requirements, for further enhancement of dynamic performance of the vehicles [1–3].

2. Requirements for Vehicle Performance and Matching of Driven Parameters

Partial transmission scheme, one of the schemes for electric vehicles, has a simple structure. It utilized a centralized driven method through a single reduction gear with constant speed ratio and limited adjustment. Within this scheme, the request for a driving cycle was completely dependent on motor speed regulation, contributing to the dynamic

underperformance of electric vehicles at medium-high speed. Hence, for a superior balance between cost and performance, the two-stage retardation method in power transmission with motor-drive integrated driving formulation has been investigated.

2.1. Technical Parameters of Electric Vehicles A Subsection. The technical parameters and design requirements of a small electric car have been listed in Table 1.

2.2. Selection and Matching of Driving Motor. Driving motor has been employed in electric cars at present, including DC motor, AC asynchronous motor, permanent-magnet synchronous machine, and switched reluctance machine. The features of those motors vary. DC motor has been used in electric vehicles at an early stage and gradually been replaced due to its complicated large structure along with frequently high-cost maintenance. Permanent-magnet synchronous machine, among the AC motors, has competitive overload capacity, with higher load efficiency and power factors than others, but inferior in constant power factor. Even though, the permanent-magnet synchronous machine, which is small in size, holds advantages of torque performance, high efficiency, and reliability was used in our study.

2.2.1. Power Matching of Driving Motor. It is known that driving motor plays a decisive role in the performance of the vehicle. Driving motors with low power cannot afford valid dynamic properties and in turn make themselves overloaded for a long time, which negatively influences their lifetime. On the other hand, high-power motors provide great reserve capability with increased mass and volume, affecting the overall efficiency of vehicles, and hence, they are not the economical option for electric cars [4–6].

To find a suitable driving motor for electric vehicles, several factors including rated output, peak power, rated revolution, and the maximum revolution, should be taken under consideration.

First, the rated output and peak power of the motor was determined, in which rated output should support the long-term steady run of the car at the highest speed. Rolling resistance and air resistance impact when cars are on the road. In accordance with those factors, under the maximum speed ($V_{\max}$), the required power of the vehicle can be calculated based on the following formula.

$$P_{V_{\max}} = \left(mgf + \frac{C_D A V_{\max}^2}{21.15}\right) \frac{V_{\max}}{3600\eta_T}. \quad (1)$$

In the formula, m represents complete vehicle curb mass (kg); g represents gravitational acceleration (m/s^2); f represents the coefficient of rolling resistance; C_D represents the coefficient of air resistance; A represents frontal area; $V_{\max}$ represents maximum speed (km/h), and η_T represents transmission efficiency.

The rated power of driving motor in electrical vehicles should be more than 90% of the required power when the vehicles driving on the horizontal road at highest speed. In another word, the minimum power for electrical vehicles to run at maximum speed on the horizontal road can be set as the minimum value of the rated power. In addition, taking the requirement from accessories of vehicles into consideration, the final calculated rated power is 20 kW and peak power is 40 kW (based on Formula (2)).

Table 1: Technical parameters of electric vehicles.

Name of parameters	Value
Complete vehicle curb mass (m)	950
Maximum loading capacity (kg)	210
Frontal area A (m^2)	1.94
The rolling radius of the tire R (m)	0.329
Transmission efficiency η_T	0.86
Coefficient of air resistance C_D	0.3
Correction coefficient of mass δ	1.04
Coefficient of rolling resistance f	0.011
Maximum speed $V_{\max}$	110 km/h
Maximum gradeability $i_{\max}$ 25 km/h	25%
Driving mileage s	150 km
Acceleration time (0-50 km/h)	8 s
Acceleration time (0-100 km/h)	14 s

Further, the peak power of the motor was determined by the $V_{\max}$, maximum gradeability and the acceleration time, which has been given in the following formula.

$$P_{mas} \geq \max\left(P_{V_{\max}}, P_{i\ \max}, P_t\right). \quad (2)$$

Apart from the rolling resistance and air resistance, grade resistance should be considered. When the stabilized speeding for climbing is 25 km/h, the related power can be calculated as per the following equation.

$$P_{i\ \max} = \left(mgf\cos\alpha_{\max} + mg\sin\alpha_{\max} + \frac{C_D A V_s^2}{21.15}\right) \frac{V_s}{3600\eta_T}. \quad (3)$$

In the equation, $\alpha_{\max}$ represents the maximum angle of gradient; V_s represents stabilized speed (km/h).

The acceleration time of the vehicle was confirmed on a horizontal road, thus, the required power for accelerating time in the absence of grade resistance can be calculated by the following equation.

$$P_t = \left(mgf + \frac{C_D A V^2}{21.15} + \delta m\frac{dv}{dt}\right) \frac{V}{3600\eta_T}. \quad (4)$$

In the equation, v represents running speed (km/h); δ represents the correction coefficient of mass.

Subsequently, the equivalent fitting has been employed to the procedure from standstill to acceleration of the vehicle, simplifying the calculation of the connection between speed and acceleration time, which has been revealed in the following equation.

$$V = V_m \left(\frac{t}{t_m}\right)^a. \quad (5)$$

In the equation, V_m indicates the speed at the end of acceleration (km/h); t_m represents accelerating time (s); a represents fit coefficient (in general, $a = 0.5$).

Equation (6) shown below can be obtained when plugging Equation (5) into Equation (4):

$$P_t = \left(mgf\frac{V_m}{1.5} + \frac{C_D A V_m^3}{52.875} + \frac{\delta m V_m^2}{7.2 t_m}\right)\frac{1}{3600\eta_T}. \quad (6)$$

In accordance with acceleration time mentioned in Table 1, 50 km/h and 100 km/h were taken as V_m separately, while 8 s and 14 s were taken as t_m, respectively. After the calculation, the power required for 0-50 km/h acceleration is 15.40 kW, whereas 37.42 kW is needed for 0-100 km/h acceleration.

Further, to sustain the highest speed, the minimum power of the motor is 15.47 kW, and also the minimum motor power for climbing is 19.21 kW. Taken together, the peak power for acceleration time is the largest among those various conditions. Based on Equation (2), the motor peak power should be no less than 37.42 kW. With a certain overload capacity, motors within electric cars have the rated power which is more than 90% of the power needed for the highest running speed on the level road [7]. In addition, attachments such as electronic devices and air conditioners consume amounts of power in the car. Thus, in this paper, we took the power required for cars running with the highest speed on the horizontal road as the lower limit for the rated power of the driving motor, which means the minimum rate power is 15.47 kW.

2.2.2. Options for Driving Motors. The permanent-magnet synchronous machines have a maximum speed from 4000 to 10000 r/min in general, belonging to medium speed motors. The coefficient of expanded power zone (β), which is around 2 to 4, has been identified by the ratio between the highest speed and rated speed of the motor. The higher the maximum speed of the driving motor, the stricter production along with higher cost would be, in which higher quality of gear and bearing units within the transmission system needs to be reinforced, especially in impact resistance and fatigue endurance [8]. Here, we set the initial rated speed of the motor as 2500 r/min, the highest speed as 8000 r/min, and β value as 3.2.

Under the condition, the rated power of the driving motor was 20 kW and peak power was 40 kW, while calculated rated torque and peak torque equaled 76 $N * m$ and 152 $N * m$, respectively. The parameters for the motor have been given in Table 2.

Table 2: Parameters of driving motor.

Parameters	Value
Rated power	20 kW
Peak power	40 kW
Rated speed	2500 r/min
Peak speed	8000 r/min
Rated torque	76 $N * m$
Peak torque	152 $N * m$

3. Design of Transmission System

3.1. Options for the Transmission Scheme. The transmission scheme of electric cars has been roughly divided into mechanical drive layout, motor-drive axle integral, and distributed layout, in which mechanical drive layout is out of date. Distributed electric drive has attracted massive attention recently; however, its further full-fledged application remains challenging. Currently, the motor-drive axle combined scheme, used in almost electric vehicles on the market, is simple in structure but with high efficiency, which exerts the similar driving performance of traditional fuel cars and has lower development cost compared to the integral scheme. Thus, it has been chosen by various companies and put on the front axle of the vehicle for cost control.

In the motor-drive combined scheme, the transmission box has several formulations, including constant speed ratio retarder and multidrive. Multidrive has increased gears, which could raise the operating time of motors while running with high efficiency, improving the dynamic and economic properties of the vehicle. Nevertheless, there is a limitation of the gears, and excessive gears complicate transmission with increased mass and cost. It is well accepted that two-speed transmission is available for existing electric vehicles, where additional gears will not bring obvious improvements of the performance other than the reduction of efficiency. Further, the transmission system directly impacts on the dynamic properties and mechanical efficiency. Therefore, the fixed speed ratio retarder, which has a simple structure, lightweight, compact size, and low cost, has been employed in current electric vehicles to slow down and increase torque. Furthermore, small electric vehicles we investigated declared low dynamic properties, while the permanent magnet synchronous motor chosen for them was equipped with excellent wide-range low-speed torque [9]. Hence in the study, to reduce the cost, the fixed speed ratio retarder has been adopted with conventional differential to make up the deceleration system. As shown in Figure 1, the double reduction was composed of four gears, in which Gear4 was integrated with the differential to reduce install size and weight. Back motion can be achieved by motor reversal. In addition, the motor was connected with a high-speed shaft through splines. For compact structure, in integrated Gear4-differential, the bevel gear of the differential was placed at the right end of Gear4 and assembled inside the retarder shell with splash lubrication.

3.2. Design of Transmission Ratio. The transmission ratio plays a pivotal role in the dynamic and economic properties of vehicles [10]. The allowed minimum and maximum transmission ratio value should be calculated, so a suitable total transmission ratio can be chosen.

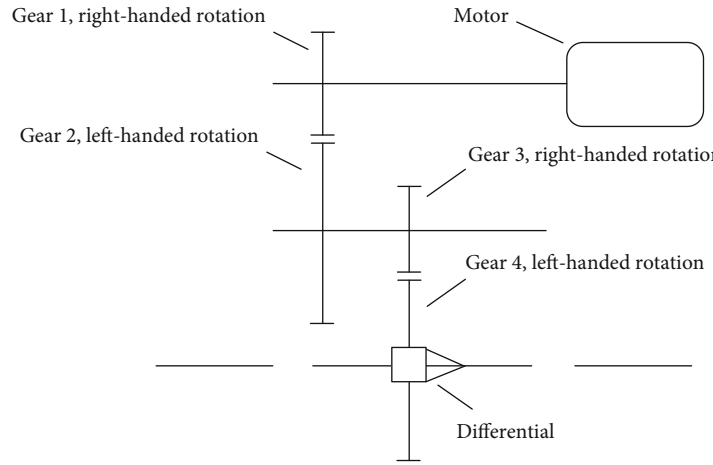

Figure 1: Two-dimension diagram of deceleration system.

The maximum transmission ratio enables vehicles to climb at a steady speed when the motor outputs the maximum torque, as shown in the following formula.

$$i_0 \cdot i_g \geq \frac{\left[mg(f\cos\alpha_{\max} + \sin\alpha_{\max}) + \left(C_D A V_s^2/21.15\right)\right]}{T_{\max} \cdot \eta_T}. \tag{7}$$

In the formula, i_0 represents transmission ratio of the main retarder, i_g represents transmission ratio of differential, r represents rolling radius of the tire (m), and $T_{\max}$ represents peak torque of motor ($N * m$). And also, in Formula (8), the maximum driving force should be no more than the adhesive rate.

$$i_0 \cdot i_g \leq \frac{F_Z \cdot \phi \cdot r}{T_{\max}\eta_T}. \tag{8}$$

In the formula, F_Z represents the normal reaction of the ground to the driving wheel, and ϕ represents the coefficient of adhesion (0.8 has been used in the study). After calculation, the range of $i_{\max}$ is from 5.987 to 9.373.

Then, minimum transmission ratio has a relation with the maximum speed and running resistance of the vehicle, which has been shown in Formula (9).

$$i_0 \cdot i_g \leq \frac{0.377r \cdot n_{\max}}{V_{\max}}. \tag{9}$$

In the formula, $n_{\max}$ represents the maximum speed of the motor, and $V_{\max}$ represents maximum speed (km/h), complied with the following formula.

$$i_0 \cdot i_g \geq \frac{\left(mgf + C_D A V_{\max}^2\right) \cdot r}{T_{\max}\eta_T}. \tag{10}$$

The estimated range for $i_{\min}$ is 1.096 to 9.021.

Taken together, the total range of the designed transmission ratio in the study has been shown in the following formula.

Table 3: Transmission parameters.

Parameters	Value
First transmission ratio	2.789
Peak power of the motor	40 kW
Peak torque of the motor	152 $N * m$
Input torque of the high-speed shaft	152 $N * m$
Input power of the high-speed shaft	40 kW
Input torque of the low-speed shaft	415.449 $N * m$
Input power of the low-speed shaft	39.20 kW

Table 4: Gear parameters for differential.

Parameters	Axle shaft gear	Planetary gear
The number of teeth	20	16
Module	3 mm	3 mm
Helix angle	51.340°	38.660°
Reference diameter	60 mm	48 mm
Gear width	12 mm	12 mm
Pressure angle	22°30'	22°30'

$$\begin{cases} 5.987 \leq i_{\max} \leq 9.373, \\ 1.096 \leq i_{\min} \leq 9.021. \end{cases} \tag{11}$$

Due to the high speed of the driving motor, a relatively small ratio of transmission should be excluded from the design. Based on the abovementioned calculation, $i_{\max}$ should be no more than 9.021 while $i_{\min}$ should be no less than 5.987. Thus, the initial transmission ratio was set as 8.1. Generally, the equal speed ratio principle was employed in the two-stage transmission ratio [11].

3.3. Design and Modeling of the Transmission Case

3.3.1. Parameter Calculation. Both first and second gear in retarder were driven by helical cylindrical gear, and their parameters have been exhibited in Table 3.

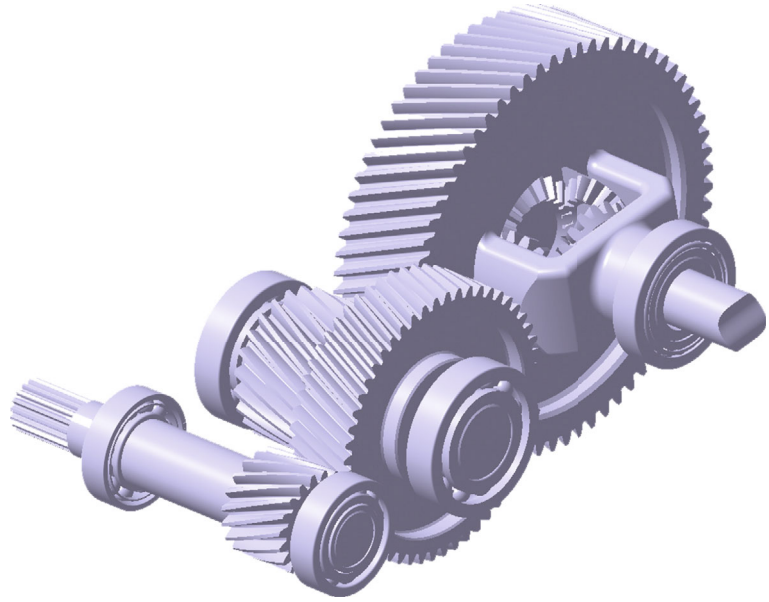

Figure 2: Structure model of the transmission case.

Figure 3: Model after web thickness reduction.

As per the design manual, the first transmission-related parameters have been examined and displayed as follows: the number of Gear 1 teeth ($z1 = 19$), the number of Gear 2 ($z2 = 53$), module (2.5 mm), center distance (97 mm), helix angle (21.90°), reference diameter of Gear 1 (51.194 mm), reference diameter of Gear 2 (142.805 mm), gear width ($b1 = 40$ mm, $b2 = 38$ mm), and transmission ratio (2.789). Similarly, second gear was driven by helical cylindrical gear, in which the number of teeth in pinion ($z3$) was 23 and in rack wheel ($z4$) was 67 along with the coefficient of face width as 0.7, followed by serious parameters including standard module ($m2 = 3.0$), center distance (146 mm), helix angle (22.392°), reference diameter of Gear 3 (74.627 mm), reference diameter of Gear 4 (217.391 mm), gear width ($b3 = 60$ mm, $b4 = 55$ mm), and transmission ratio (2.913).

In accordance with the bearing requirement of small electric vehicles, the planetary gear number was set as 2. The spherical radius of planetary gear (Rb) can be roughly determined by empirical in the following formula.

$$R_b = K_b \sqrt[3]{T_d}. \tag{12}$$

In the formula, T_d represents calculated torque of differential, K_b represents spherical radius coefficient of planetary gear, and $K_b = 3.0$ has been taken in the study. Added, R_b

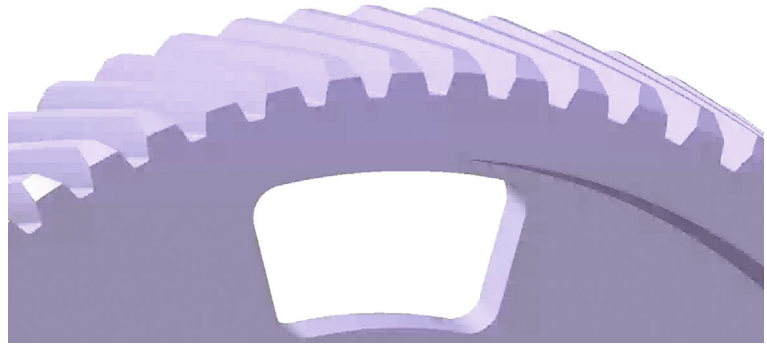

Figure 4: Structure of the through-hole.

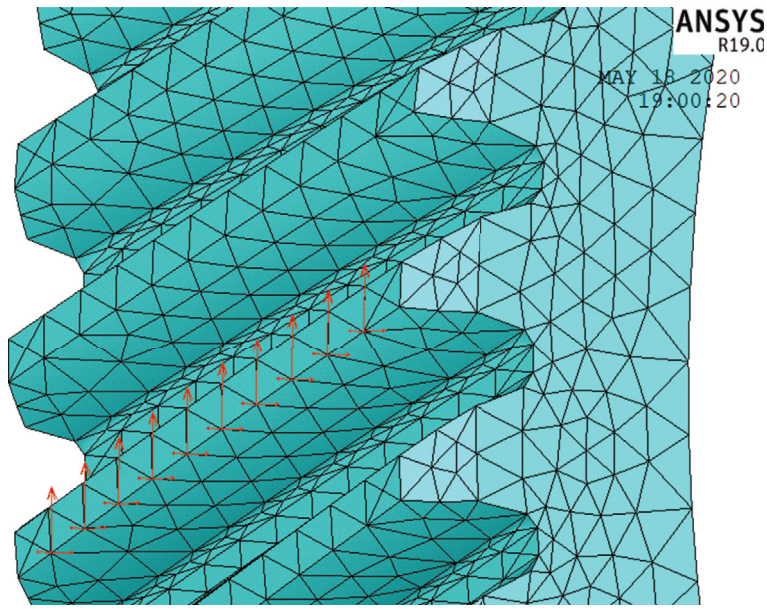

Figure 5: Position of applied force.

was set as 31.744 mm, and thus, pitch cone of planetary gear (A_0) might be 31.11 mm and 31.43 mm based on the equation $A_0 = (0.98 \sim 0.99)/R_b$. The differential was connected directly to the final output axis, which has been identified as an axle shaft, under large torque force, and thus, greater module ($m = 3$ mm) was adopted for assurance of strength. Generally, the teeth number of planetary gear ($z1$) should be no less than 10, whereas the teeth number of axle shaft gear ($z2$) should be between 14 to 25, with a teeth ratio ($z2/z1$) between 1.5 and 2.0 [12]. For engagement of those four bevel gears simultaneously, the number of their teeth should be even ($z1 = 16$, $z2 = 20$, shown in Table 4).

20CrMnTi has been well studied as the conventional materials used in vehicles' gearbox shafts. Here, we reported the design and examination of the important units of retarder, including high-speed shaft, low-speed shaft, transmission gears, bearing units, and other retarder components, to make sure the reliable strength under the motor's maximum torque output. As the high-speed shaft was designed to have a straightforward connection with the motor, the minimum diameter of the high-speed shaft was defined as 30 mm while 40 mm for the low-speed shaft in diameter.

3.3.2. Modeling of the Driving System. The model of retarder assembled by CATIA has been shown in Figure 2.

4. Light-Weight Design of Transmission Case

Driving mileage has a decisive impact on the development of electric vehicles, whose weight in turn influences their driving mileage. Hence, under the condition of safety concerns, utilization of advanced materials along with novel technology could cut down the weight of the car, extending the vehicle's driving mileage, which could also improve the dynamic and economic properties by saving materials and resources. As has been exhibited in Figure 2, Gear 4, the biggest gear in the transmission case, reached 12.725 kg in weight, whose light-weight design holds particular significance.

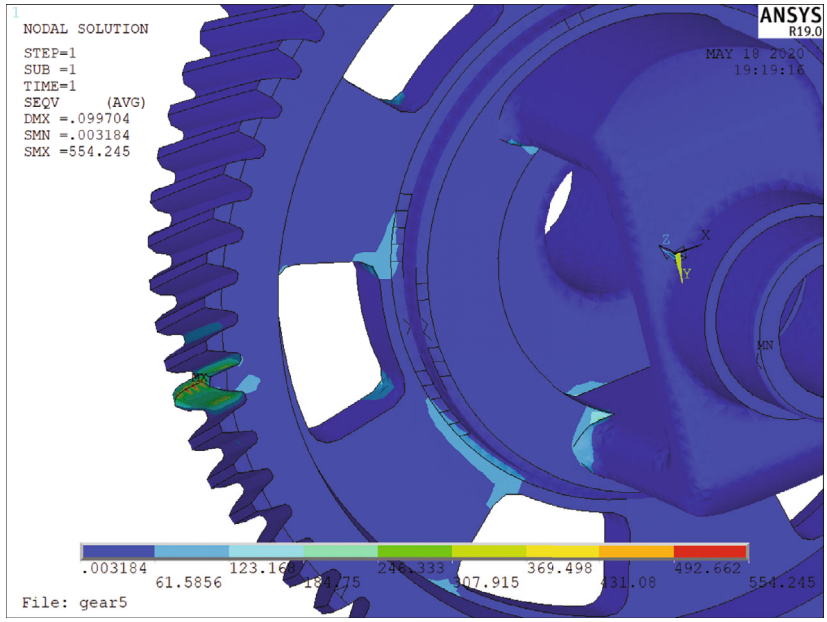

Figure 6: Simulated stress nephogram.

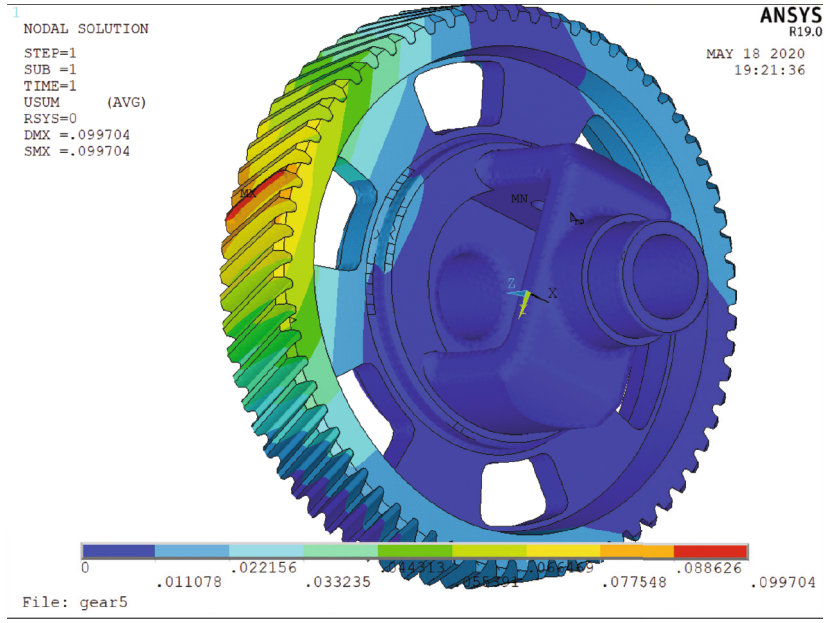

Figure 7: Simulated displacement nephogram.

4.1. Method for Light-Weight Design. Conventional mechanical design has been used in the gears. In other words, root bending fatigue limit and contact fatigue limit of tooth surface provided the basis of gear design, in which excessive safety coefficient leads to much more redundancy in gear size [1]. 20CrMnTi, used in the study, has a considerable high tensile strength of more than 1080 MPa, offering opportunities for size optimization. Gears comprise hub, rim, and web in common. However, due to the presence of differential, Gear 4 did not have the structure of hub, and also chances for light-weight improvement of differential are less. Further, the rim of the gear was determined by its basic parameters, which has been almost fixed in structure. Therefore, the optimization was focused on Gear 4 [13] by reduction of coefficient of gear width followed with spoke type improvement.

In the transmission case, the initial coefficient of face width was 0.7 and the face width was 55 mm. And the target coefficient of face width and the face width was 0.56 and 44 mm, respectively. Under the circumstance, in accordance with the conventional gear design, the corresponding reference diameter of Gear 3, which was engaged

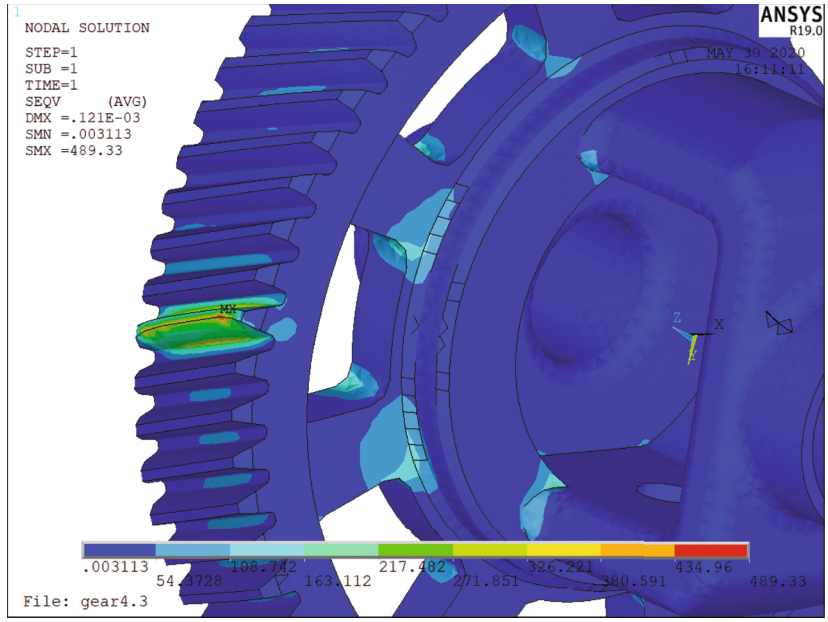

Figure 8: Simulated stress nephogram.

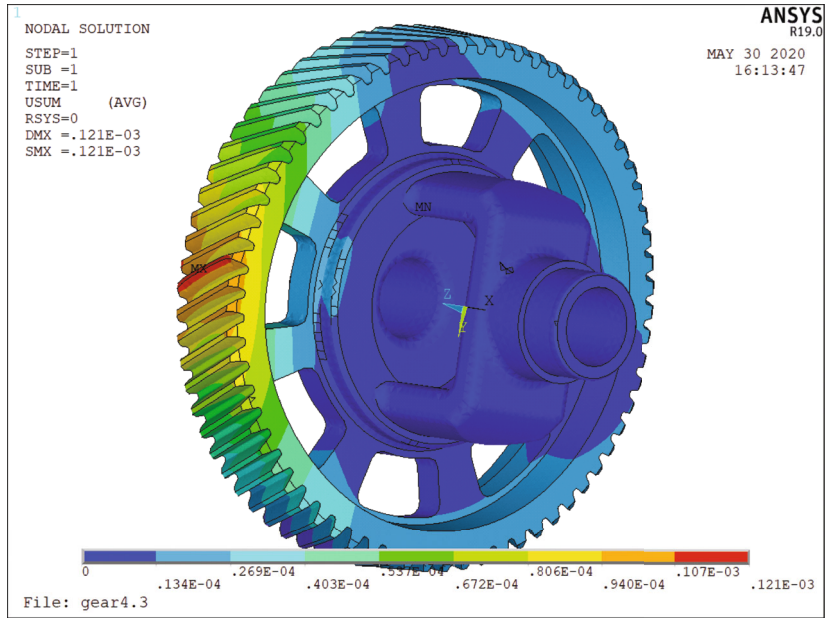

Figure 9: Simulated displacement nephogram.

with Gear 4, should be more than 42.35 mm following by module (more than 2.192 mm). So, the gear reached the strength requirements.

Hence, in the study, the main work of the optimization was to improve and examine the spoke type of Gear 4 for light-weight design.

4.2. Light-Weight Design of Gear Structure. Due to concern of the structure, the optimization design of the overall transmission system is mainly carried on Gear 4, which has the largest weight proportion, by reducing the tooth width coefficient and optimizing the spoke structure. The principle of optimal design contains two parts. One side, the strength should meet the requirement. On the other side, there is no possibility of resonance when transmission gears are working after modal analysis. Therefore, lightweight design, in which FEM from ANSYS was used to analyze the gradually optimized structure, has been applied in the optimization of gear structure. The main process was as follows:

(1) *Thickness Reduction of the Web.* Regularly, gear structure can be divided into several types, including solid, web, and spoke type. As has been mentioned in Section 3.3.1, the reference diameter for Gear 4 was 217.4 mm, and the web type was used. As per the manual of mechanical design, the thickness of the

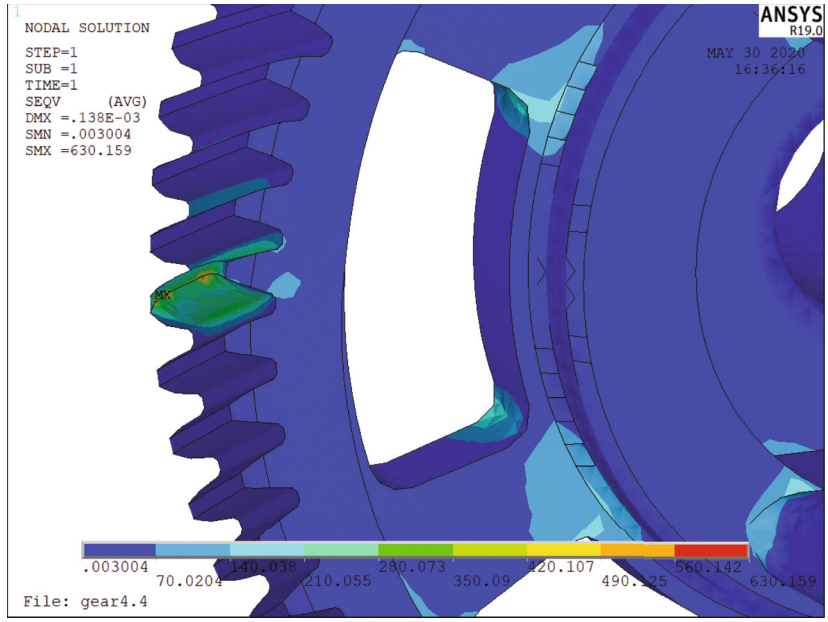

Figure 10: Simulated stress nephogram.

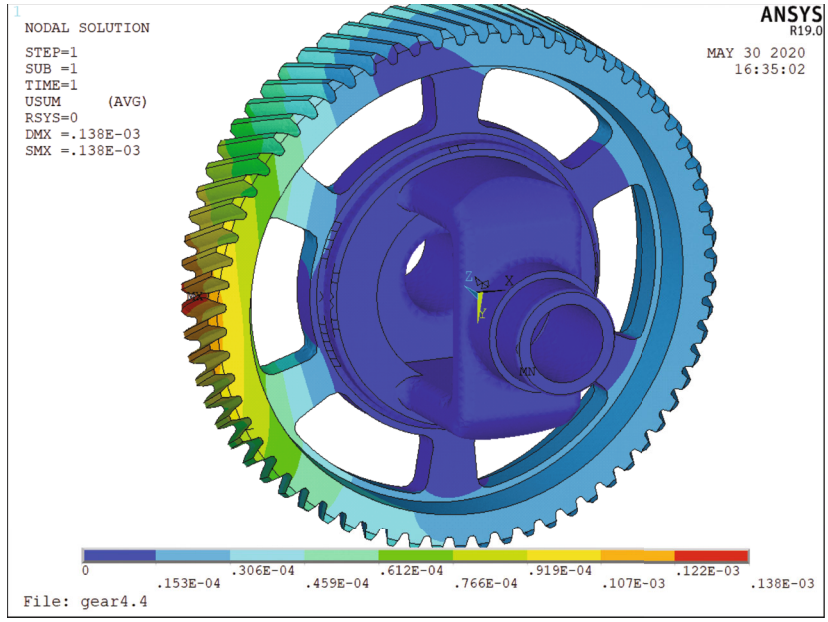

Figure 11: Simulated displacement nephogram.

web should be no less than 10 mm. Therefore, based on references, 13 mm of thickness was defined. The structure was shown in Figure 3

(2) *Optimization of Web Topology*. In general, topological optimization indicates the investigation of best material distribution scheme, which could bear the load, within the design area. Thus, the stress distribution on the web of the gear under the working condition could be quickly determined through topological optimization, from which the optimized scheme could be picked. In another word, the proportion in system for light-weight optimization could be confirmed. Therefore, few steps should be followed. The finite element model should be set up firstly, followed by gear material selection. Then, the corresponding load can be applied to the model with settled boundary conditions, and the topology optimized results can be achieved in Ansys/Workbench. Huang and colleagues analyzed gear topology optimization based on Ansys/Workbench. The outward of those gears' web was reported to have

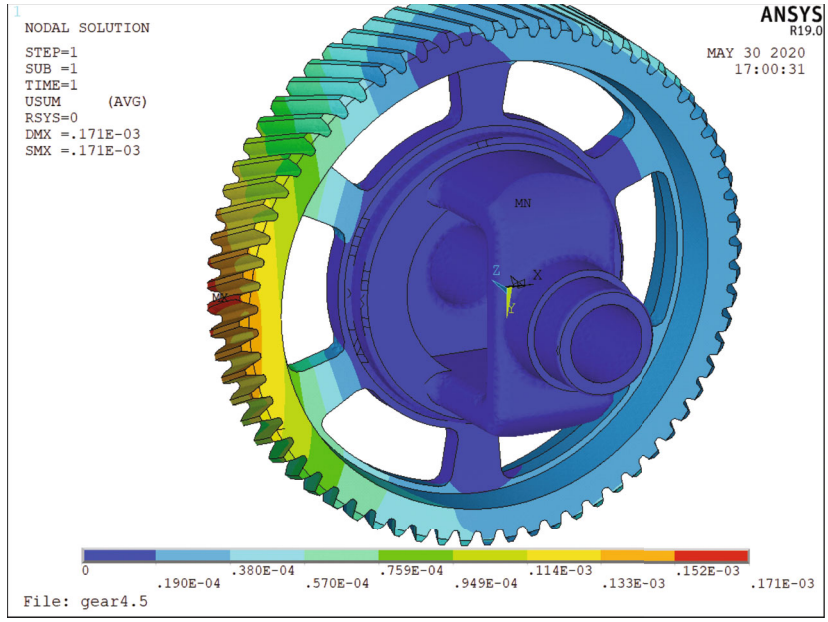

Figure 12: Simulated stress and displacement nephogram.

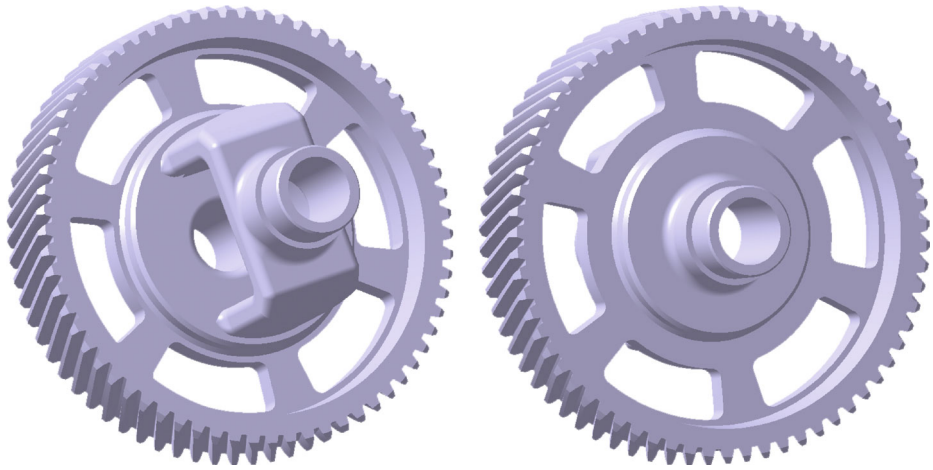

Figure 13: Optimized structure of Gear 4.

considerable residual strength, which could be hollowed out for light-weight purposes [14]. In addition, the equivalent stress on spoke-plate gears was less compared to circular hole structures with the same material. Taken together, six through-holes were made on the outward of the web at first. The area of a single through-hole was 9.932 cm^2, while the total area of the through-hole was 59.592 cm^2. The specific structure has been displayed in Figure 4

Based on the analysis of dedendum bending stress, the peak stress of gear engagement emerged at the place of through holes. Thus, mesh division was applied to the model, followed by circumferential force, radial force, and axial force on the addendum circle of the through-hole (Figure 5).

In Figure 6, the acceptable maximum stress (554 MPa) appeared on the tooth surface, which is within the limit contact stress of 20CrMnTi (745 MPa). However, in Gear 4, at the root of differential shell and inner ring of the web, stress concentration came up with the value around 130 MPa, indicating the further improvement could be achieved considering the materials' features. Nevertheless, in Figure 7, the maximum displacement (0.0997 mm) took place on the tooth surface where force was applied, confirmed to safety standards.

Table 5: Modal frequency of nonupdated Gear 4.

Oder	Intrinsic frequency (Hz)
1	901.23
2	1492.5
3	1924.4
4	2307.3
5	2314.9
6	2351.1

Table 6: Modal frequency of updated Gear 4.

Oder	Intrinsic frequency (Hz)
1	1103.4
2	1208.5
3	1342.7
4	1668.1
5	1768.6
6	1797.2

As has been mentioned above, the stress on the web was far less than the limit when there were six through-holes, thus, more through-holes (up to eight) were further studied. The total area of eight through holes reached 79.456 cm^2, and the corresponding simulated stress and displacement nephogram has been exhibited in Figures 8 and 9, respectively.

It is shown that the stress is employed mainly on the inner ring with the maximum value of 163 MPa (Figure 8). In comparison with the six-through-hole structure, the stress on the inner ring increased in this updated safe 8-through-hole model. Inconsistent with the results, the maximum displacement augmented to 0.121 mm (Figure 9). Compared to the earlier one, the whole structure enlarged.

For manufacturing and technological feasibility, decreased number of through-holes with the increased area was authorized. In the simulation, the number of through-holes decreased to 6, and the single area of those holes increased to 15.004 cm^2. The total area of through-holes was 90.024 cm^2, larger than what has mentioned in the eight-through-hole structure.

Under the same condition, the maximum stress increased up to 210 MPa within the web (Figure 10) whereas the maximum displacement reached 0.138 mm (Figure 11). This newly light-weighted structure confirmed the strength requirement.

(3) Later, the thickness of the web was reduced to a critical size of 10 mm referred to the design manual. As displayed in Figure 12, no significant enhancement of maximum stress was shown on the web, while the area under large force was raised. On the other hand, the maximum displacement increased by 0.171 mm after the thickness reduction. However, the gear deformation should be no more than 0.15 mm on account of engineering experience and mechanical design manual. In this way, the present designed structure underwent a rather large displacement. Hence, the thickness of web was determined as 13 mm

Taken together, the finalized structure of Gear 4 has been shown in Figure 13. In CATIA, its mass was measured and shown as 7.498 kg, which was 41% of the previous design.

4.3. Modal Analysis of Gear Optimization. The intrinsic frequency has been determined by the structure of the gear. Thus, the probability of the occurrence of resonance in light-weighted Gear 4 during work has been analyzed.

In the beginning, the prior six modes of the initially designed structure in Gear 4 have been analyzed, in which all the degrees of freedom at bearing positions were restricted. And the relative modal frequency has been listed in Table 5, while the same feature examined in the updated structure has been exhibited in Table 6.

Compared with the nonupdated structure, the relevant modal frequency had few differences. Interestingly, obvious diversity in mode of vibration was shown in the last three modes. The first-stage intrinsic frequency was raised, while others declined to some extent but within the safety zone, which will not induce resonance normally.

5. Conclusion

In summary, this study investigated the structure of the transmission system in small electric vehicles and optimized the gear in retarder, one of the units for the transmission system, by reducing 20% of face width along with a novel spoke structure. Also, the finite element method was used to analyze the strength of gear structure for safety concerns. The total weight of the initial design was 12.725 kg, of which roughly 41% of weight has been diminished based on CATIA analysis. Thus, the final weight reached 7.489 kg, and the safe light-weight target was achieved perfectly [15].

In the future, further following investigations can be processed. One side, optimizing the overall structure of the transmission case by utilizing novel materials and manufacturing technology to further cut down its weight. On the other side, particular updates, especially the improvement of the device structure, can be processed on transmission structure within the transmission case. By approaching the demand for transmission power, the model system could be established to enhance the efficiency of the transmission case for better choices [16].

Data Availability

The datasets used and/or analyzed during the current study are available from the corresponding author on reasonable request.

Conflicts of Interest

It is declared by the authors that this article is free of conflict of interest.

Acknowledgments

The study presented in this article was substantially supported by Natural Science Foundation of China (no. 51505172). The supports are gratefully acknowledged.

References

[1] J. Shen, S. L. Zheng, and J. Z. Feng, "Light weight design of gear sets in wheel driving deceleration system of electric vehicle

based on load spectrum," *Journal of Mechanical Strength.*, vol. 39, no. 4, pp. 835–841, 2017.

[2] G. X. Zhao, *Research on Electric Vehicle Powertrain Matching and Global Optimization*, Jiangsu University, 2017.

[3] C. W. Huang, S. L. Zheng, J. Z. Feng, and J. Shen, "Lightweight design of gear webs in wheel-side deceleration system of electric vehicle," *Agricultural Equipment & Vehicle Engineering.*, vol. 55, no. 4, pp. 1–5, 2017.

[4] X. Y. Xu, "Developement of transmission technology for energy-saving vehicles and new energy resource vehicle," *Journal of Automotive Safety and Energy.*, vol. 8, no. 4, pp. 323–332, 2017.

[5] C. J. Liang, "Analysis of the influence of transmission system on the performance of electric vehicles," *Shanghai Auto.*, vol. 9, p. 4-8+27, 2018.

[6] B. H. Zhang, *Parameter matching design and optimization of power system for pure electric*, Chongqing Jiaotong University, 2017.

[7] J. Li, *Paremeters Design and Optimization of Powertrain for Battery Electric Vehicle*, Chang'an University, 2017.

[8] J. H. Liu, "Matching design of powertrain parameters of pure electric vehicle. Auto," *Manufacturing Engineering*, vol. 3, p. 57-58+61, 2018.

[9] J. M. Wang, *Design and optimization of driving system of battery electric vehicle*, Jilin University., 2019.

[10] Z. S. Yu, *Automobile Theory*, China Mechine Press, Beijing, Edition 5 edition, 2009.

[11] L. Wang, *Structure Design and Anylsis of Pure Electric Vehicle Gear Box*, Jilin University, 2015.

[12] W. Y. Wang, *Automobile Design. Edition 4*, China Mechine Press, Beijing, 2004.

[13] C. Zou, "Research on gear lightweight based on ANSYS workbench," *Mechanical Engineering*, vol. 5, pp. 34–36, 2015.

[14] Y. Li, *Simulation and Design Method Research of Large Gear Lightweight of Ball Mill*, Northeastern University, 2013.

[15] P. D. Walker and S. A. Rahman, *Modelling, simulations, and optimisation of electric vehicles for analysis of transmission ratio selection*, Hindawi Publishing Corporation., 2013.

[16] J. J. Hu and H. L. Ran, "Parameter design and performance analysis of shift actuator for a two-speed automatic mechanical transmission for pure electric vehicles," *Advances in Mechanical Engineering*, vol. 8, no. 8, 2016.